

Anisotropic g -Factor and Spin-Orbit Field in a Ge Hut Wire Double Quantum Dot

Ting Zhang,^{1,2, #} He Liu,^{1,2, #} Fei Gao,^{3, #} Gang Xu,^{1,2} Ke Wang,^{1,2} Xin Zhang^{1,2}, Gang Cao,^{1,2} Ting Wang,³ Jianjun Zhang,³ Xuedong Hu⁴, Hai-Ou Li,^{1,2,*} and Guo-Ping Guo^{1,2,5,*}

¹ CAS Key Laboratory of Quantum Information, University of Science and Technology of China, Hefei, Anhui 230026, China

² CAS Center for Excellence and Synergetic Innovation Center in Quantum Information and Quantum Physics, University of Science and Technology of China, Hefei, Anhui 230026, China

³ Institute of Physics and CAS Center for Excellence in Topological Quantum Computation, Chinese Academy of Sciences, Beijing 100190, China

⁴ Department of Physics, University at Buffalo, SUNY, Buffalo, New York 14260, USA

⁵ Origin Quantum Computing Company Limited, Hefei, Anhui 230026, China

[#]These authors contributed equally to this work

* Corresponding author. Emails: haiouli@ustc.edu.cn (H.-O. L.); gpguo@ustc.edu.cn (G.-P.G.).

Abstract

Holes in nanowires have drawn significant attention in recent years because of the strong spin-orbit interaction, which plays an important role in constructing Majorana zero modes and manipulating spin-orbit qubits. Here, from the strongly anisotropic leakage current in the spin blockade regime for a double dot, we extract the full g -tensor and find that the spin-orbit field is in plane with an azimuthal angle of 59° to the axis of the nanowire. The direction of the spin-orbit field indicates a strong spin-orbit interaction along the nanowire, which may have originated from the interface inversion asymmetry in Ge hut wires. We also demonstrate two different spin relaxation mechanisms for the holes in the Ge hut wire double dot: spin-flip cotunneling to the leads, and spin-orbit interaction within the double dot. These results help establish feasibility of a Ge-based quantum processor.

Keywords: *Ge hut wires, hole double quantum dot, Pauli spin blockade, spin-orbit interaction, g -tensor*

Main text

The spin-orbit interaction (SOI) can be considered as a coupling between the momentum of a carrier and its spin. When an electron or hole moves in an electric field, it experiences an effective magnetic field that couples to its spin degree of freedom, even in the absence of an external magnetic field¹⁻³. Recently, studies on the SOI have received widespread attention because of its fundamental role in both classical spintronics and the quantum coherent manipulation of a spin qubit⁴⁻¹⁹, and more recently in the search for Majorana fermions²⁰⁻²⁵. The SOI can be exploited for all-electrical manipulation of a spin-orbit qubit using electric dipole spin resonance (EDSR) techniques^{4-19,26-31}. Without generating a local ac magnetic field or making use of an external source of spin-electric coupling (such as micromagnets), the device design is simplified by using a local ac electric field. In addition, as proposed by theory and confirmed by recent experiments, a strong SOI is required to create Majorana fermions in semiconductor-superconductor heterostructures^{20-25,32,33}. Thus, the potential applications of the SOI for quantum information processing will be particularly relevant in the future, especially with respect to fast operation speed³¹, scalability³⁴, and topological quantum computation³⁵.

At the mean field level, SOI can be characterized with an effective magnetic field \vec{B}_{SO} . Here, the amplitude of \vec{B}_{SO} reflects the strength of the SOI, which is related to the Rabi frequency in EDSR³¹, and the direction of \vec{B}_{SO} determines the suitable geometries in experimental setups. For example, the special geometry $\vec{B} \perp \vec{B}_{\text{SO}}$ is assumed in proposals for realizing Majorana fermions in nanowires with proximity-induced superconductivity^{32,33}. Furthermore, EDSR is efficient when the externally applied magnetic field \vec{B} is perpendicular to \vec{B}_{SO} ³⁶⁻³⁸. However, under such conditions, the degree of mixing between the singlet and triplet states in a double quantum dot also reaches a maximum, which is expected to be proportional to $|\vec{B}_{\text{SO}} \times (\vec{B}/B)|$ ³⁹⁻⁴¹. The transitions between T(1,1) and S(0,2) induced by the SOI hybridization have an adverse

effect on the fidelity of the initialization and readout of spin qubits^{39,42-44}, and could speed up decoherence⁴⁵⁻⁵².

Holes in Ge hut wires (HWs)⁵³ are recognized as a prospective platform for quantum computation because of their favourable properties. The extremely strong “direct Rashba spin-orbit interaction” (DRSOI)⁵⁴⁻⁵⁶ in Ge HWs enables a fast Rabi frequency of 540 MHz¹⁸, which is the record manipulation speed for semiconductor spin qubits up to now. Furthermore, the growth of site-controlled Ge HWs has been demonstrated recently³⁴, which opens a potential path towards large-scale multi-qubit device fabrication. To establish the feasibility of hole-based quantum processors, and to possibly observe novel phenomena such as the Majorana zero mode in Ge HWs, it is imperative to investigate the spin-orbit field (SOF), in terms of both its magnitude and its direction.

To date, by analysing the anisotropic effects of the SOI, the SOF direction has been determined in various semiconducting nanostructures such as hole quantum dots (QDs) in the GaAs/AlGaAs heterostructure⁴³, silicon MOS^{57,58}, and electron QDs made from InAs nanowires⁵⁹. However, experimental determination of the SOF direction, which is related to the DRSOI in hole nanowires, remains lacking.

In this letter, we extract the anisotropic g -tensor and determine the SOF direction in an electrostatically defined double quantum dot (DQD) in a Ge hut wire by analysing the behavior of leakage in the Pauli spin blockade (PSB) region. First, we measure the dependence of leakage current on the magnetic field along different directions, which can be attributed to the relaxation mechanisms of spin-flip cotunneling to the reservoirs and SOI within the DQD. The effective g -factors in-plane can be determined by fitting to the current peak induced by spin-flip cotunneling. Then, the magnetic field is fixed at a value dominated by the SOI. We study the anisotropic effects of the leakage current and extract the direction of \vec{B}_{SO} , which is in-plane and at a 59° angle to the nanowire, indicating the existence of other SOI mechanisms in addition to the DRSOI.

The DQD used in the experiment is fabricated from Ge HWs that are monolithically grown on a Si substrate⁵³. Figure 1a shows a false-coloured scanning

electron microscopy (SEM) image of the device we studied with five electrodes above a 1- μm -long nanowire. After removing oxides with buffered hydrofluoric acid, 30-nm-thick palladium contacts are patterned with electron beam lithography. A 20-nm aluminium oxide layer is then deposited as a gate dielectric using atomic layer deposition. Finally, three 30-nm-wide top gates consisting of 3-nm titanium and 25-nm palladium are fabricated between contact pads, spaced at a 40 nm pitch. A 3D schematic of the device is depicted in Figure 1b. By applying voltages to three top gates to create a confinement potential, a DQD is defined along the y -axis (parallel to the Ge HW), as shown in Figure 1c. Here, the experiment is carried out in a dilution refrigerator at a base temperature of about 15 mK.

Figure 1d shows the charge stability diagram of the DQD. We measure the source-drain current I_{SD} as a function of gate voltages V_L and V_R at a bias voltage $V_{\text{SD}} = +2.5$ mV. Note that only when the energy levels corresponding to transitions of the two QDs both enter the bias window can the current through the DQD be detected, leading to an array of characteristic bias triangles^{51,60}. We investigate the bias triangle denoted by a red circle at the transition between the (1,1) and (0,2) states in Figure 1d. Here, the number in parentheses describes the effective hole occupation of each quantum dot, while the true hole occupation is (m+1, n+1) and (m, n+2). When the total hole spin of each dot is zero in the (m,n) state, the spin-related transition between (m+1, n+1) and (m, n+2) states can be described with (1,1) and (0,2) states for simplicity. Figures 2a and 2b display zoom-ins of this triangle for positive and negative source-drain biases. The corresponding line traces along the detuning energy ε (green arrow) are plotted in Figure 2c. In comparison, we observe a strong suppression of current at $V_{\text{SD}} = +2.5$ mV, which is attributed to the forbidden transition from T(1,1) to S(1,1) due to spin conservation during hole tunneling (Figure 2d), the characteristic signature of PSB⁶¹⁻⁶⁵. For $V_{\text{SD}} = -2.5$ mV, a large current is measured in the whole triangle.

The spin blockade can be lifted by spin relaxation mechanisms such as hyperfine interaction^{62,67,68}, spin-flip cotunneling^{66,69-71}, a g -factor difference in the DQD and the SOI^{39,44,67,69,72}. The dominant spin relaxation mechanism can be determined based on

the leakage current in the PSB region. Figure 3 shows a measurement of the leakage spectroscopy as a function of ε and \vec{B} in different directions. Here, ε can be tuned by changing the voltages of gates L and R as described in Figure 2a (green arrow), and the direction of \vec{B} is depicted on the top panels of Figure 3. Figure 3a shows the leakage spectroscopy when the magnetic field is along the z direction. The leakage current I_{SD} in the PSB region increases monotonically as B_z increases. A line cut along $\varepsilon = 0$ is plotted (red circles) in Figure 3d. The PSB is lifted at a finitely large magnetic field, and the current profile shows a broad dip, reflecting the presence of a spin-nonconserving transport mechanism. In Ge HWs, the strong SOI can hybridize the states of T(1,1) and S(0,2) at a finite magnetic field and enable a spin-flip transition between them to lift the PSB³⁹, leading to the leakage spectroscopy shown in Figure 3a.

However, when the direction of magnetic field is rotated perpendicularly and parallelly to the nanowire in plane, we find a different field-dependent behaviour of the leakage current, as shown in Figures 3b and 3c. From the line cut at $\varepsilon = 0$ (Figures 3e and 3f), we find the leakage curve is composed of a zero-field peak and a dip at a large magnetic field, which is induced by two different spin relaxation mechanisms. We attribute the broad leakage dip to the SOI in our system and find that the current increment induced by the SOI with an in-plane magnetic field is much smaller than that with an out-of-plane magnetic field. Although no saturation of leakage current is observed as before⁴³, we find that the dip widths are dramatically different in different directions. This phenomenon can be explained with the anisotropy of the g -factor in our hole system and the change in the angle between \vec{B} and \vec{B}_{SO} ⁴³, which will be discussed in detail below.

Furthermore, because the width of the peak is approximately 200 mT, we rule out the hyperfine interaction^{62,68} and consider spin-flip cotunneling^{66,69} to be the dominant mechanism for lifting of the PSB around zero field. When a triplet T(1,1) is formed in a DQD, one of the spins can flip through inelastic cotunneling between the dot and its nearest lead, giving rise to an enhanced leakage current. The spin-flip cotunneling rate

will decrease exponentially with the increase of Zeeman energy⁶⁶. Therefore, the leakage current induced by spin-flip cotunneling has a maximum at zero field and drops to zero at a large magnetic field, leading to a peak of leakage current

The leakage current I_{leak} induced by SOI and spin-flip cotunneling can be expressed by^{39,69}

$$I_{\text{leak}} = \frac{4ecg^*\mu_B B}{3\sinh\frac{g^*\mu_B B}{k_B T}} + I_{\text{SO}}^0 \frac{B^2}{B^2 + B_C^2} + I_B, \quad (1)$$

The first term in the formula describes the contribution from the spin-flip cotunneling, with $c = \frac{h}{\pi} [\{\Gamma_L/\Delta\}^2 + \{\Gamma_R/(\Delta - 2U_M - 2eV_{\text{SD}})\}^2]$, where e is the hole charge, g^* is the effective g -factor, μ_B is the Bohr magneton, h is Plank's constant, k_B is the Boltzmann constant, T is the hole temperature, $\Gamma_{L(R)}$ is the tunnel coupling with the left (right) reservoir, Δ is the depth of the two-hole level, and U_M is the mutual charging energy⁷¹. The second term in the formula represents the SOI induced leakage current, which exhibits a Lorentzian-shaped dip with a width B_C ³⁹. And the residual leakage current I_B results from other spin relaxation mechanisms, such as the difference of g -factor between two dots.

The black solid lines in Figures 3d-3f show the fitting to experimental data of the leakage current at $\varepsilon = 0$ with eq (1). Obviously, the experimental data are in good agreement with the theory. From the fitting to the current peak induced by spin-flip cotunneling, we can extract the values of the effective g -factor $g_x^* = g_y^* = 1.2 \pm 0.2$ with a hole temperature $T = 40$ mK. The obtained g -factors for a magnetic field applied in-plane are consistent with those previously extracted for a single QD⁷³. By fitting the data in Figures 3d-3f in three different directions and focusing on the SOI part of eq (1), we can extract the values of B_C , with $B_C^x = 9$ T, $B_C^y = 6.5$ T and $B_C^z = 1.7$ T. The values of B_C are so large that they exceed the limit of the magnetic field we can reach, which is why we cannot observe saturation of the leakage current induced by the SOI at a finite field. Here, B_C is related not only to the effective g -factor but also to the angle between $\hat{g} \cdot \vec{B}$ and \vec{B}_{SO} , and it can be expressed as^{43,57}

$$B_C = \frac{B_C^0}{g^* \sin \alpha}, \quad (2)$$

where B_C^0 is a constant, g^* is the effective g -factor along the direction of magnetic field and α is the angle between \vec{B}_{SO} and $\hat{g} \cdot \vec{B}$; here, \hat{g} is the g -tensor. The g -factor in Ge HW has been demonstrated to be extremely anisotropic, with $g_\perp > g_\parallel$ ⁷³, leading to a much smaller B_C along the z -axis, which is consistent with our experimental result.

To systematically study the anisotropy spectroscopy and determine the SOF direction, a fixed magnetic field is rotated in the x - y , x - z , and y - z planes while the leakage is measured in the PSB region. Figure 4 shows the leakage current as a function of detuning energy ε and rotation angle in three orthogonal planes with a fixed magnetic field of 0.8 T, where spin-flip cotunneling is completely suppressed and the SOI dominates. Combining eq (1) and eq (2), the leakage current I_{leak} induced by the SOI can be expressed by

$$I_{\text{leak}} = I_{\text{SO}}^0 \frac{B^2}{B^2 + \left(\frac{B_C^0}{g^* \sin \alpha}\right)^2} + I_B'. \quad (3)$$

Based on the g -factor in the plane we obtained above, the g -tensor for holes in our DQD is well approximated by

$$\hat{g} \approx \begin{pmatrix} 1.2 & 0 & 0 \\ 0 & 1.2 & 0 \\ 0 & 0 & g_z \end{pmatrix}, \quad (4)$$

where g_z is the g -factor along the z -direction. Considering the effect of SOI in our system, the Rashba SOI will produce a correction to the in-plane g -factor and the Dresselhaus SOI will lead to an off-diagonal element g_{xy} , which is proportional to the spread of the wave function in the z -direction⁷⁴. Because of the strong out-of-plane confinement in our system (the height of Ge HW is around 2 nm), we expect that the value of g_{xy} should be less than 0.1, which is much smaller than the larger diagonal elements and take it as zero for simplicity. Hence, the effective g -factor along the external magnetic field can be expressed by

$$g^*(\varphi, \theta) = \sqrt{\hat{r}^\dagger(\varphi, \theta) \hat{g}^\dagger \hat{g} \hat{r}(\varphi, \theta)}, \quad (5)$$

where

$$\hat{r}^\dagger(\varphi, \theta) = (\sin\theta\cos\varphi, \sin\theta\sin\varphi, \cos\theta) \quad (6)$$

is a unit vector pointing along the magnetic field direction. The angle α between \vec{B}_{SO} and $\hat{g} \cdot \vec{B}$ can also be expressed based on the g -tensor \hat{g} and the direction of \vec{B} , \vec{B}_{SO} .

Figures 4d-4f show the leakage current measured at $\varepsilon = 0$, which changes periodically with the angle of the magnetic field. From the theoretical expression of eq (3), the extreme anisotropy in the leakage current induced by the SOI in Figure 4 can be explained by two different processes: when the magnetic field is rotated in the x - z , y - z plane, the experimental results in Figures 4a and 4b are caused by the high anisotropy of g -factor in Ge HWs⁷³. In our system, the effective g -factor reaches its maximum (minimum) when the field points perpendicular (parallel) to the substrate of the nanowires, leading to a minimum (maximum) of B_C and a maximum (minimum) of I_{leak} , as shown in eq (3), which is consistent with our experimental results in Figures 4d and 4e. When the magnetic field is rotated in the x - y plane (Figure 4c), the angle between \vec{B} and \vec{B}_{SO} changes, which affects the degree of hybridization of T(1,1) and S(1,1)³⁹⁻⁴¹. Especially when the angle between \vec{B} and \vec{B}_{SO} reaches a minimum (i.e., \vec{B} is aligned with the projection of \vec{B}_{SO} in-plane), the spin-flip tunnelling induced by the SOI is suppressed the most, leading to a minimum leakage current in Figure 4f.

To accurately determine the direction of the SOF \vec{B}_{SO} , we simultaneously perform numerical fitting of the leakage current measured in three orthogonal planes with eq (3). The red solid lines in Figures 4d-4f represent the theoretical fits according to eq (3) and show great agreement with our experimental results. From these fits, we can extract the SOF direction, which corresponds to $(\theta_0, \varphi_0) = (90^\circ \pm 10^\circ, 31^\circ \pm 5^\circ)$, and the value of $g_z = 3.9 \pm 0.1$. The g -tensor we extracted is consistent with ones obtained in the literature before⁷³. The ground state in Ge HWs is expected to be an almost pure heavy-hole (HH) state with a very small light-hole (LH) admixture (less than 1%). However,

the PSB we studied here is in the region of multiple holes in the QD. This finite occupation should increase the HH-LH mixing and lead to an increase in g_{\parallel} and a decrease in g_{\perp} , which agrees well with the experimental results in ref 73. Compared to other one-dimensional systems such as Ge/Si core/shell nanowires, a significant feature of the Ge HWs studied here is their triangular cross-section⁵³. The lack of inversion symmetry of the cross-section can lead to a large intrinsic SOI that is dependent on the orientation of the wire even without external electric fields⁷⁵. Because the wires grow horizontally along either the [100] or [010] direction⁵³, the intrinsic SOF points in the x -direction according to the theoretical model in ref 75. Notably, the interface inversion asymmetry can also contribute to the SOI^{2,76-78}. A Dresselhaus SOI may exist in our system due to the anisotropy of the chemical bonds at material interfaces⁷⁶. Including the spin-orbit terms we mentioned above, the DRSOI, interface SOI and intrinsic SOI induced by the asymmetry of the cross-section, the SOI Hamiltonian in our system can be described by

$$H_{\text{SO}} = \alpha k_y \sigma_x + \beta k_y \sigma_y. \quad (7)$$

Here, α is the Rashba interaction coefficient, which accounts for the effect of the DRSOI and intrinsic SOI, β is the Dresselhaus interaction coefficient, which corresponds to the interface SOI, k_y is the hole wave operator along the wire, and σ_x and σ_y are the Pauli spin matrices. Hence, the direction of the SOF in our system can be expressed as $(\alpha, \beta, 0)$, and we can extract the ratio between the Rashba and Dresselhaus SOI in our system $\beta/\alpha = \tan 31^\circ \approx 0.6$. Because the DRSOI is related to the electric field^{55,56}, the direction of the SOF \vec{B}_{SO} can be adjusted by the gate voltages we apply. The existence of Dresselhaus SOI in our system makes it possible to find operational sweet spots⁷⁵ where decoherence effect from charge noise is reduced. By controlling the growth of nanowires along different crystal directions, we can completely turn off SOI when two types of SOI are of equal strength but with opposite directions, realizing the persistent spin helix symmetry³.

In conclusion, we have measured the leakage current through a DQD in Ge HWs in the PSB regime. We observe and distinguish two different PSB lifting mechanisms:

spin-flip cotunneling and SOI, which lead to an increase in the leakage current. When rotating the direction of magnetic field, we observe the high anisotropy of the leakage current induced by the SOI and explain the experimental results with a combination of the anisotropic hole g -factor and the angle between \vec{B}_{SO} and $\hat{g} \cdot \vec{B}$. By analysing the behavior of the leakage current anisotropy, the direction of the SOF \vec{B}_{SO} is determined and found to be in-plane with an azimuthal angle of 59° to the nanowire, indicating a large interface SOI along the nanowire. The results we obtained may inspire future developments in the operation of spin qubits and the detection of Majorana fermions.

Acknowledgements

This work was supported by the National Key Research and Development Program of China (Grant No.2016YFA0301700), the National Natural Science Foundation of China (Grants No. 12074368, 61674132, 12034018, 11625419 and 61922074), the Strategic Priority Research Program of the CAS (Grant No. XDB24030601), the Anhui initiative in Quantum Information Technologies (Grants No. AHY080000), X. H. acknowledge financial support by U.S. ARO through No. W911NF1710257, and this work was partially carried out at the USTC Center for Micro and Nanoscale Research and Fabrication.

References

- (1) Bliokh, K. Y.; et al. Spin–orbit interactions of light. *Nat. Photonics*. **2015**, *9*, 796-808.
- (2) Winkler, R. *Spin-Orbit Coupling Effects in Two-Dimensional Electron and Hole Systems*. Springer Tracts Mod. Phys. Vol. 191 (Springer, Berlin, 2003).
- (3) Sasaki, A.; Nonaka, S.; Kunihashi, Y.; Kohda, M.; Bauernfeind, T.; Dollinger, T.; Richter, K.; Nitta, J. Direct determination of spin-orbit interaction coefficients and realization of the persistent spin helix symmetry. *Nat. Nanotechnol.* **2014**, *9*, 703-709.
- (4) Buluta, I.; et al. Natural and artificial atoms for quantum computation. *Rep. Prog. Phys.* **2011**, *74*, 104401.
- (5) Nakajima, T.; et al. Coherent transfer of electron spin correlations assisted by dephasing noise. *Nat. Commun.* **2018**, *9*, 2133.
- (6) Lambert, N.; et al. Amplified and tunable transverse and longitudinal spin-photon coupling in hybrid circuit-QED. *Phys. Rev. B: Condens. Matter Mater. Phys.* **2018**, *97*, 125429.
- (7) Hu, X.; et al. Strong coupling of a spin qubit to a superconducting stripline cavity. *Phys. Rev. B: Condens. Matter Mater. Phys.* **2012**, *86*, 035314.
- (8) Giavaras, G.; et al. Transport spectroscopy of a spin-orbit-coupled spin to a quantum dot. *Phys. Rev. B: Condens. Matter Mater. Phys.* **2016**, *94*, 155419.
- (9) Fan, J.; et al. Electric-field-induced interferometric resonance of a one-dimensional spin-orbit-coupled electron. *Sci. Rep.* **2016**, *6*, 38851.
- (10) Nowack, K. C.; Koppens, F. H. L.; Nazarov, Yu. V.; Vandersypen, L. M. K. Coherent Control of a Single Electron Spin with Electric Fields. *Science* **2007**, *318*, 1430-1433.
- (11) van den Berg, J. W. G.; Nadj-Perge, S.; Pribiag, V. S.; Plissard, S. R.; Bakkers, E. P. A. M.; Frolov, S. M.; Kouwenhoven, L. P. Fast Spin-Orbit Qubit in an Indium Antimonide Nanowire. *Phys. Rev. Lett.* **2013**, *110*, 066806.
- (12) Nadj-Perge, S.; Frolov, S. M.; Bakkers, E. P. A. M.; Kouwenhoven, L. P. Spin-orbit qubit in a semiconductor nanowire. *Nature* **2010**, *468*, 1084-1087.

- (13) Watzinger, H.; Kukučka, J.; Vukušić, L.; Gao, F.; Wang, T.; Schäffler, F.; Zhang, J. J.; Katsaros, G. A germanium hole spin qubit. *Nat. Commun.* **2018**, *9*, 3902.
- (14) Maurand, R.; Jehl, X.; Kotekar-Patil, D.; Corna, A.; Bohuslavskiy, H.; Laviéville, R.; Hutin, L.; Barraud, S.; Vinet, M.; Sanquer, M.; De Franceschi, S. A CMOS silicon spin qubit. *Nat. Commun.* **2016**, *7*, 13575.
- (15) Hendrickx, N. W.; Franke, D. P.; Sammak, A.; Scappucci, G.; Veldhorst, M. Fast two-qubit logic with holes in germanium. *Nature* **2020**, *577*, 487-491.
- (16) Hendrickx, N. W.; Lawrie, W. I. L.; Petit, L.; Sammak, A.; Scappucci, G.; Veldhorst, M. A single-hole spin qubit. *Nat. Commun.* **2020**, *11*, 3478.
- (17) Scappucci, G.; Kloeffer, C.; Zwanenburg, F. A.; Loss, D.; Myronov, M.; Zhang, J. J.; De Franceschi, S.; Katsaros, G.; Veldhorst, M. The germanium quantum information route. *Nat. Rev. Mater.* **2020**, <https://doi.org/10.1038/s41578-020-00262-z>.
- (18) Wang, K.; Xu, G.; Gao, F.; *et al.* Ultrafast Operations of a Hole Spin Qubit in Ge Quantum Dot. *arXiv:2006.12340*, Jun 22, **2020**. arXiv.org e-Print archive. <https://arxiv.org/abs/2006.12340> (accessed Apr 20, **2021**).
- (19) Froning, F. N. M.; Camenzind, L. C.; van der Molen, O. A. H.; Li, A.; Bakkers, E. P. A. M.; Zumbühl, D. M.; Braakman, F. R. Ultrafast Hole Spin Qubit with Gate-Tunable Spin-Orbit Switch. *Nat. Nanotechnol.* **2021**, *16*, 308-312.
- (20) Mourik, V.; Zuo, K.; Frolov, S. M.; Plissard, S. R.; Bakkers, E. P. A. M.; Kouwenhoven, L. P. Signatures of Majorana Fermions in Hybrid Superconductor-Semiconductor Nanowire Devices. *Science* **2012**, *336*, 1003-1007.
- (21) Das, A.; Ronen, Y.; Most, Y.; Oreg, Y.; Heiblum, M.; Shtrikman, H. Zero-bias peaks and splitting in an Al-InAs nanowire topological superconductor as a signature of Majorana fermions. *Nat. Phys.* **2012**, *8*, 887-895.
- (22) Das Sarma, S.; Freedman, M.; Nayak, C. Majorana zero modes and topological quantum computation. *npj Quantum Inf.* **2015**, *1*, 15001.
- (23) Finck, A. D. K.; *et al.* Anomalous modulation of a zero-bias peak in a hybrid nanowire-superconductor device. *Phys. Rev. Lett.* **2013**, *110*, 126406.
- (24) You, J. Q.; *et al.* Encoding a qubit with Majorana modes in superconducting

circuits. *Sci. Rep.* **2014**, *4*, 5535.

(25) Zhang, P.; et al. Coherent manipulation of a Majorana qubit by a mechanical resonator. *Phys. Rev. B: Condens. Matter Mater. Phys.* **2015**, *92*, 115303.

(26) Pioro-Ladrière, M.; Obata, T.; Tokura, Y.; Shin, Y.-S.; Kubo, T.; Yoshida, K.; Taniyama, T.; Tarucha, S. Electrically driven single-electron spin resonance in a slanting Zeeman field. *Nat. Phys.* **2008**, *4*, 776-779.

(27) Tokura, Y.; van der Wiel, W. G.; Obata, T.; Tarucha, S. Coherent Single Electron Spin Control in a Slanting Zeeman Field. *Phys. Rev. Lett.* **2006**, *96*, 047202.

(28) Laird, E. A.; Barthel, C.; Rashba, E. I.; Marcus, C. M.; Hanson, M. P.; Gossard, A. C. Hyperfine-Mediated Gate-Driven Electron Spin Resonance. *Phys. Rev. Lett.* **2007**, *99*, 246601.

(29) Bednarek, S.; Pawłowski, J.; Skubis, A. Manipulation of a single electron spin in a quantum dot without magnetic field. *Appl. Phys. Lett.* **2012**, *100*, 203103.

(30) Nadj-Perge, S.; Pribiag, V. S.; van den Berg, J. W. G.; Zuo, K.; Plissard, S. R.; Bakkers, E. P. A. M.; Frolov, S. M.; Kouwenhoven, L. P. Spectroscopy of Spin-Orbit Quantum Bits in Indium Antimonide Nanowires. *Phys. Rev. Lett.* **2012**, *108*, 166801.

(31) Li, R.; You, J. Q.; Sun, C. P.; Nori, F. Controlling a Nanowire Spin-Orbit Qubit via Electric-Dipole Spin Resonance. *Phys. Rev. Lett.* **2013**, *111*, 086805.

(32) Lutchyn, R. M.; Sau, J. D.; Das Sarma, S. Majorana Fermions and a Topological Phase Transition in Semiconductor-Superconductor Heterostructures. *Phys. Rev. Lett.* **2010**, *105*, 077001.

(33) Oreg, Y.; Refael, G.; von Oppen, F. Helical Liquids and Majorana Bound States in Quantum Wires. *Phys. Rev. Lett.* **2010**, *105*, 177002.

(34) Gao, F.; et al. Site-Controlled Uniform Ge/Si Hut Wires with Electrically Tunable Spin–Orbit Coupling. *Adv. Mater.* **2020**, *32*, 1906523.

(35) Lutchyn, R. M.; et al. Majorana zero modes in superconductor-semiconductor heterostructures. *Nat. Rev. Mater.* **2018**, *3*, 52-68.

(36) Rashba, E. I.; Efros, A. L. Orbital Mechanisms of Electron-Spin Manipulation by an Electric Field. *Phys. Rev. Lett.* **2003**, *91*, 126405.

- (37) Golovach, V. N.; Borhani, M.; Loss, D. Electric-dipole-induced spin resonance in quantum dots. *Phys. Rev. B: Condens. Matter Mater. Phys.* **2006**, *74*, 165319.
- (38) Flindt, C.; Sorensen, A. S.; Flensberg, K. Spin-Orbit Mediated Control of Spin Qubits. *Phys. Rev. Lett.* **2006**, *97*, 240501.
- (39) Danon, J.; Nazarov, Y. V. Pauli spin blockade in the presence of strong spin-orbit coupling. *Phys. Rev. B: Condens. Matter Mater. Phys.* **2009**, *80*, 041301.
- (40) Nowak, M. P.; Szafran, B.; Peeters, F. M.; Partoens, B.; Pasek, W. J. Tuning of the spin-orbit interaction in a quantum dot by an in-plane magnetic field. *Phys. Rev. B: Condens. Matter Mater. Phys.* **2011**, *83*, 245324.
- (41) Stepanenko, D.; Rudner, M.; Halperin, B. I.; Loss, D. Singlet-triplet splitting in double quantum dots due to spin-orbit and hyperfine interactions. *Phys. Rev. B: Condens. Matter Mater. Phys.* **2012**, *85*, 075416.
- (42) Bohuslavskyi, H.; Kotekar-Patil, D.; Maurand, R.; Corna, A.; Barraud, S.; Bourdet, L.; Hutin, L.; Niquet, Y.-M.; Jehl, X.; De Franceschi, S.; Vinet, M.; Sanquer, M.; Pauli blockade in a few-hole PMOS double quantum dot limited by spin-orbit interaction. *Appl. Phys. Lett.* **2016**, *109*, 193101.
- (43) Wang, D. Q.; Klocan, O.; Hung, J. T.; Culcer, D.; Farrer, I.; Ritchie, D. A.; Hamilton, A. R. Anisotropic Pauli Spin Blockade of Holes in a GaAs Double Quantum Dot. *Nano Lett.* **2016**, *16*, 7685-7689.
- (44) Li, R.; Hudson, F. E.; Dzurak, A. S.; Hamilton, A. R. Pauli Spin Blockade of Heavy Holes in a Silicon Double Quantum Dot. *Nano Lett.* **2015**, *15*, 7314-7318.
- (45) Hu, Y.; Kuemmeth, F.; Lieber, C. M.; Marcus, C. M. Hole spin relaxation in Ge-Si core-shell nanowire qubits. *Nat. Nanotechnol.* **2012**, *7*, 47-50.
- (46) Higginbotham, A. P.; Larsen, T. W.; Yao, J.; Yan, H.; Lieber, C. M.; Marcus, C. M.; Kuemmeth, F. Hole Spin Coherence in a Ge/Si Heterostructure Nanowire. *Nano Lett.* **2014**, *14*, 3582-3586.
- (47) Vukušić, L.; Kukučka, J.; Watzinger, H.; Milem, J. M.; Schäffler, F.; Katsaros, G. Single-Shot Readout of Hole Spins in Ge. *Nano Lett.* **2018**, *18*, 7141-7145.

- (48) Khaetskii, A. V.; Nazarov, Yu. V. Spin-flip transitions between Zeeman sublevels in semiconductor quantum dots. *Phys. Rev. B: Condens. Matter Mater. Phys.* **2001**, *64*, 125316.
- (49) Golovach, V. N.; Khaetskii, A. V.; Loss, D. Phonon-Induced Decay of the Electron Spin in Quantum Dots. *Phys. Rev. Lett.* **2004**, *93*, 016601.
- (50) Stano, P.; Fabian, J. Theory of Phonon-Induced Spin Relaxation in Laterally Coupled Quantum Dots. *Phys. Rev. Lett.* **2006**, *96*, 186602.
- (51) Hanson, R.; Kouwenhoven, L. P.; Petta, J. R.; Tarucha, S.; Vandersypen, L. M. K. Spins in few-electron quantum dots. *Rev. Mod. Phys.* **2007**, *79*, 1217.
- (52) Maier, F.; Kloeffel, C.; Loss, D. Tunable g factor and phonon-mediated hole spin relaxation in Ge/Si nanowire quantum dots. *Phys. Rev. B: Condens. Matter Mater. Phys.* **2013**, *87*, 161305(R).
- (53) Zhang, J. J.; Katsaros, G.; Montalenti, F.; Scopece, D.; Rezaev, R. O.; Mickel, C.; Rellinghaus, B.; Miglio, L.; De Franceschi, S.; Rastelli, A.; Schmidt, O. G. Monolithic Growth of Ultrathin Ge Nanowires on Si(001). *Phys. Rev. Lett.* **2012**, *109*, 085502.
- (54) Luo, J. W.; Li, S. S.; Zunger, A. Rapid Transition of the Hole Rashba Effect from Strong Field Dependence to Saturation in Semiconductor Nanowires. *Phys. Rev. Lett.* **2017**, *119*, 126401.
- (55) Kloeffel, C.; Trif, M.; Loss, D. Strong spin-orbit interaction and helical hole states in Ge/Si nanowires. *Phys. Rev. B: Condens. Matter Mater. Phys.* **2011**, *84*, 195314.
- (56) Kloeffel, C.; Rančić, M. J.; Loss, D. Direct Rashba spin-orbit interaction in Si and Ge nanowires with different growth directions. *Phys. Rev. B: Condens. Matter Mater. Phys.* **2018**, *97*, 235422.
- (57) Marx, M.; Yoneda, J.; Gutiérrez-Rubio, Á.; *et al.* Spin-orbit field in a physically-defined p-type MOS silicon double quantum dot. *arXiv:2003.07079*, Mar 18, **2020**. arXiv.org e-Print archive. <https://arxiv.org/abs/2003.07079> (accessed Apr 20, **2021**).
- (58) Zhang, X.; *et al.* Giant Anisotropy of Spin Relaxation and Spin-Valley Mixing

in a Silicon Quantum Dot. *Phys. Rev. Lett.* **2020**, *124*, 257701.

(59) Wang, J. Y.; Huang, G. Y.; Huang, S. Y.; Xue, J. H.; Pan, D.; Zhao, J. H.; Xu, H. Q. Anisotropic Pauli Spin-Blockade Effect and Spin-Orbit Interaction Field in an InAs Nanowire Double Quantum Dot. *Nano Lett.* **2018**, *18*, 4741-4747.

(60) van der Wiel, W. G.; De Franceschi, S.; Elzerman, J. M.; Fujisawa, T.; Tarucha, S.; Kouwenhoven, L. P. Electron transport through double quantum dots. *Rev. Mod. Phys.* **2002**, *75*, 1.

(61) Ono, K.; Austing, D. G.; Tokura, Y.; Tarucha, S. Current Rectification by Pauli Exclusion in a Weakly Coupled Double Quantum Dot System. *Science* **2002**, *297*, 1313–1317.

(62) Koppens, F. H. L.; Folk, J. A.; Elzerman, J. M.; Hanson, R.; van Beveren, L. H. W.; Vink, I. T.; Tranitz, H. P.; Wegscheider, W.; Kouwenhoven, L. P.; Vandersypen, L. M. K. Control and Detection of Singlet-Triplet Mixing in a Random Nuclear Field. *Science* **2005**, *309*, 1346-1350.

(63) Johnson, A. C.; Petta, J. R.; Marcus, C. M.; Hanson, M. P.; Gossard, A. C. Singlet-triplet spin blockade and charge sensing in a few-electron double quantum dot. *Phys. Rev. B: Condens. Matter Mater. Phys.* **2005**, *72*, 165308.

(64) Ono, K.; et al. Hole Spin Resonance and Spin-Orbit Coupling in a Silicon Metal-Oxide-Semiconductor Field-Effect Transistor. *Phys. Rev. Lett.* **2017**, *119*, 156802.

(65) Ono, K.; et al. Quantum Interferometry with a g-Factor-Tunable Spin Qubit. *Phys. Rev. Lett.* **2019**, *122*, 207703.

(66) Lai, N. S.; Lim, W. H.; Yang, C. H.; Zwanenburg, F. A.; Coish, W. A.; Qassemi, F.; Morello, A.; Dzurak, A. S. Pauli Spin Blockade in a Highly Tunable Silicon Double Quantum Dot. *Sci. Rep.* **2011**, *1*, 110.

(67) Nadj-Perge, S.; Frolov, S. M.; van Tilburg, J. W. W.; Danon, J.; Nazarov, Y. V.; Algra, R.; Bakkers, E. P. A. M.; Kouwenhoven, L. P. Disentangling the effects of spin-orbit and hyperfine interactions on spin blockade. *Phys. Rev. B: Condens. Matter Mater. Phys.* **2010**, *81*, 201305(R).

- (68) Jouravlev, O. N.; Nazarov, Y. V. Electron Transport in a Double Quantum Dot Governed by a Nuclear Magnetic Field. *Phys. Rev. Lett.* **2006**, *96*, 176804.
- (69) Brauns, M.; Ridderbos, J.; Li, A.; Bakkers, E. P. A. M.; van der Wiel, W. G.; Zwanenburg, F. A. Anisotropic Pauli spin blockade in hole quantum dots. *Phys. Rev. B: Condens. Matter Mater. Phys.* **2016**, *94*, 041411(R).
- (70) Qassemi, F.; Coish, W. A.; Wilhelm, F. K. Stationary and Transient Leakage Current in the Pauli Spin Blockade. *Phys. Rev. Lett.* **2009**, *102*, 176806.
- (71) Coish, W. A.; Qassemi, F. Leakage-current line shapes from inelastic cotunneling in the Pauli spin blockade regime. *Phys. Rev. B: Condens. Matter Mater. Phys.* **2011**, *84*, 245407.
- (72) Zarassi, A.; Su, Z.; Danon, J.; Schwenderling, J.; Hocevar, M.; Nguyen, B. M.; Yoo, J.; Dayeh, S. A.; Frolov, S. M. Magnetic field evolution of spin blockade in Ge/Si nanowire double quantum dots. *Phys. Rev. B: Condens. Matter Mater. Phys.* **2017**, *95*, 155416.
- (73) Watzinger, H.; Kloeffer, C.; Vukušić, L.; Rossell, M. D.; Sessi, V.; Kukučka, J.; Kirchschrager, R.; Lausecker, E.; Truhlar, A.; Glaser, M.; Rastelli, A.; Fuhrer, A.; Loss, D.; Katsaros, G. Heavy-Hole States in Germanium Hut Wires. *Nano Lett.* **2016**, *16*, 6879-6885.
- (74) Tantt, T.; et al. Controlling Spin-Orbit Interactions in Silicon Quantum Dots Using Magnetic Field Direction. *Phys. Rev. X.* **2019**, *9*, 021028.
- (75) Bosco, S.; Hetényi, B.; Loss, D. Hole Spin Qubits in Si FinFETs With Fully Tunable Spin-Orbit Coupling and Sweet Spots for Charge Noise. *PRX Quantum.* **2021**, *2*, 010348.
- (76) Golub, L. E.; Ivchenko, E. L. Spin splitting in symmetrical SiGe quantum wells. *Phys. Rev. B: Condens. Matter Mater. Phys.* **2004**, *69*, 115333.
- (77) Nestoklon, M. O.; Ivchenko, E. L.; Jancu, J.-M.; Voisin, P. Electric field effect on electron spin splitting in SiGe/Si quantum wells. *Phys. Rev. B: Condens. Matter Mater. Phys.* **2008**, *77*, 155328.
- (78) Prada, M.; Klimeck, G.; Joynt, R. Spin-orbit splittings in Si/SiGe quantum

wells: from ideal Si membranes to realistic heterostructures. *New Journal of Physics*.
2011, *13*, 013009.

Figure Captions :

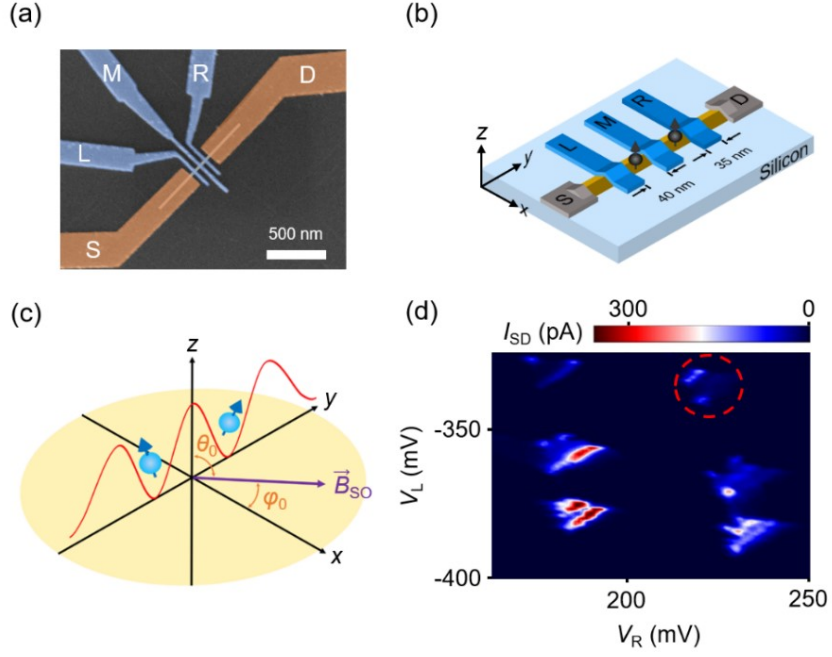


Figure 1. (a) False-coloured scanning electron microscopy (SEM) image of a hole DQD in a Ge HW. (b) A 3D schematic of the device. The DQD is formed between two top gates by applying voltages to three grid electrodes. (c) Schematic of the confinement potential created along the nanowire by a gate voltage and the formation of a DQD. Definition of the angles and presentation of the vector for the SOF. (d) Charge stability diagram of the DQD: transport current I_{SD} measured as a function of V_L and V_R with $V_{\text{SD}} = 2.5$ mV. The experiment is performed in the bias triangle circled in red.

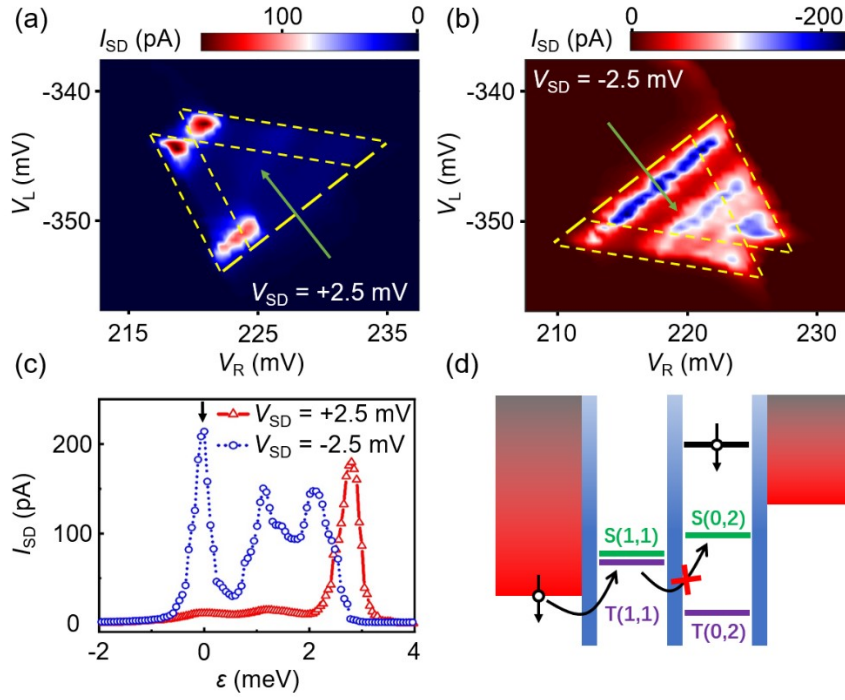


Figure 2. (a-b) The zoom-ins of the bias triangle circled in red in Figure 1d with opposite biases. The suppression of current I_{SD} at the base of the bias triangle in panel a is the signature of PSB. The green arrow indicates the direction of the detuning energy ϵ . (c) The current is measured along the detuning energy with opposite biases (d) Schematic diagram of PSB in a hole DQD. The transport between states (1,1) and (0,2) is forbidden when $T(1,1)$ is occupied.

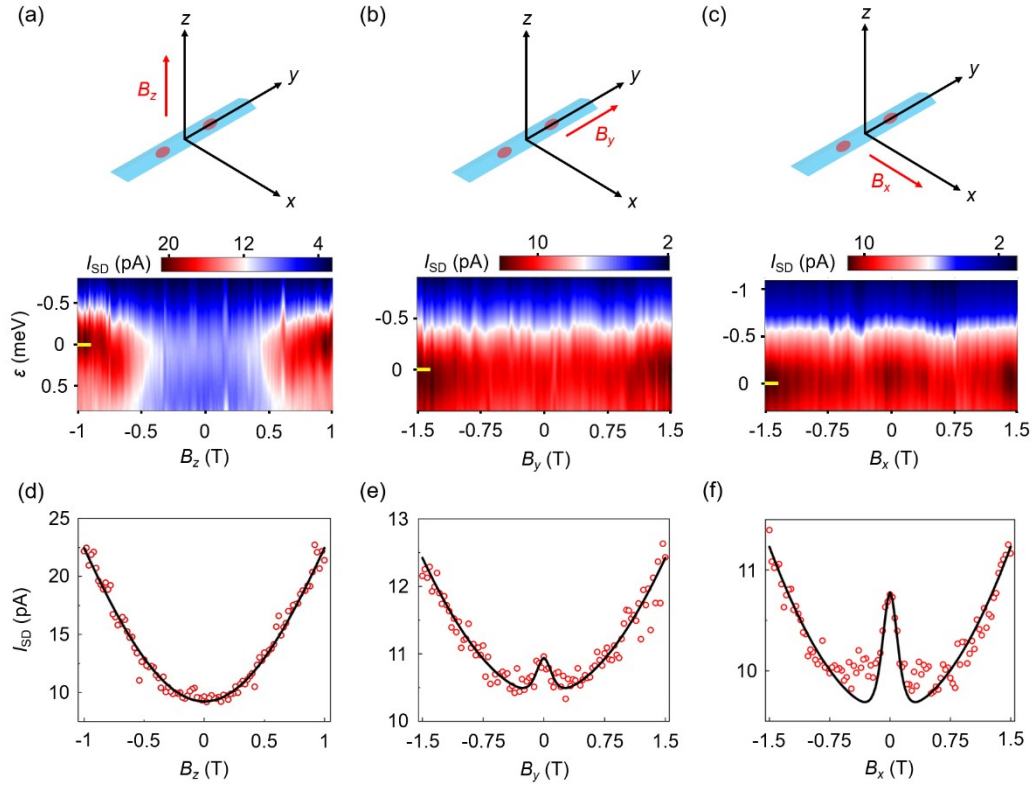


Figure 3. (a-c) The measurement of leakage spectroscopy as a function of ε and \vec{B} in different directions. The direction of magnetic field is depicted in the top panels. The Ge HW is along the y-axis. (d-f) The magnetic field dependence of leakage current along three different directions at $\varepsilon = 0$ (indicated by the yellow bars). The black solid lines represent the theoretical fits of eq (1).

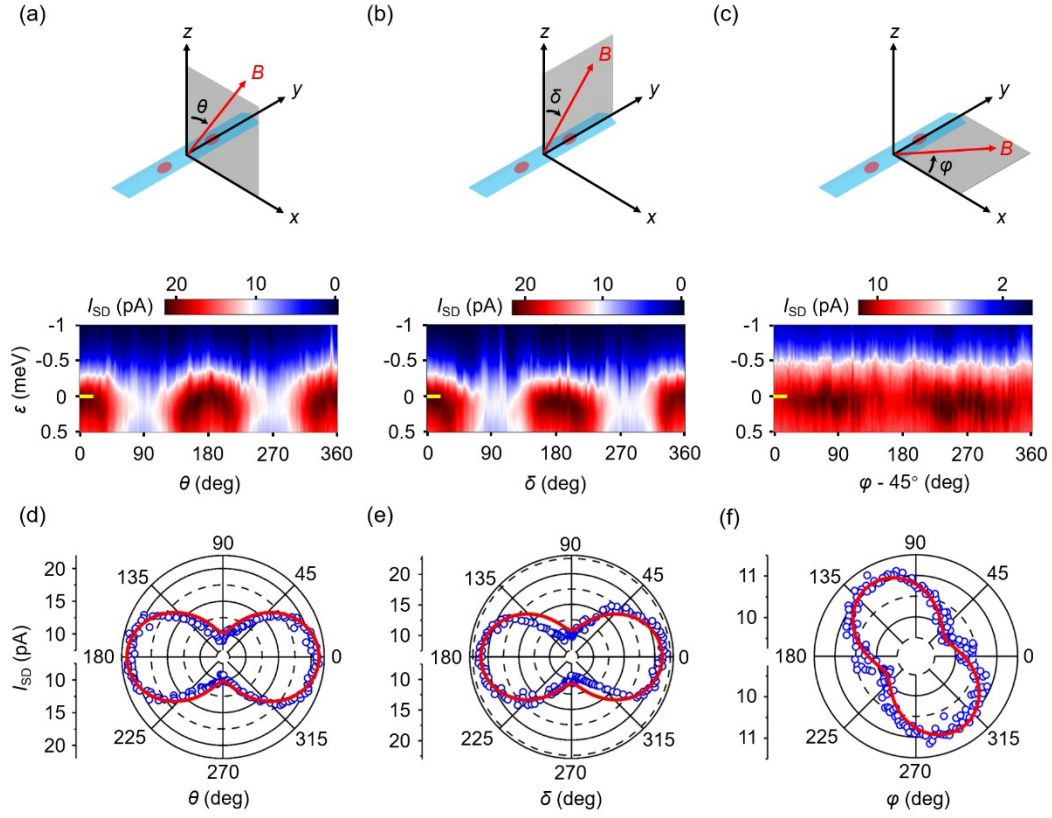
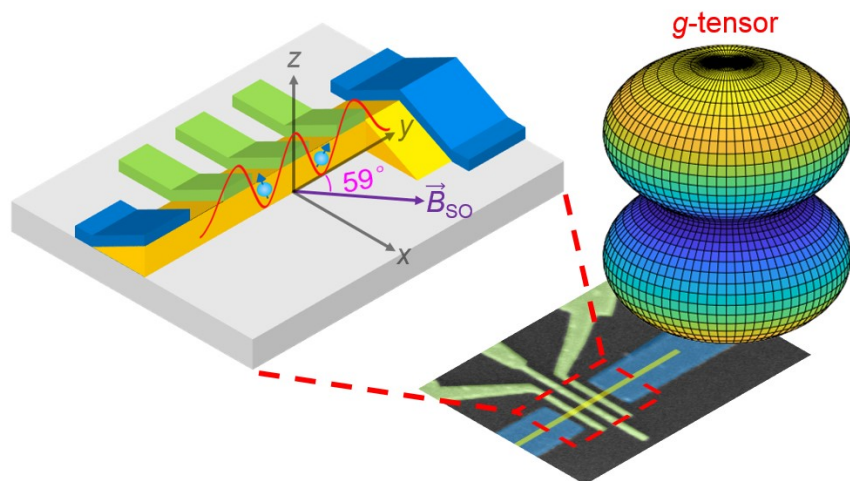


Figure 4. (a-c) The anisotropy spectroscopy of leakage current I_{SD} as a function of the detuning energy ϵ and the direction of the magnetic field which is rotated in three orthogonal planes as illustrated in the top panel. (d-f) The leakage current as a function of the magnetic field angle at $\epsilon = 0$ (indicated by the yellow bars) in three different planes. The red solid lines represent the theoretical fits of eq (3).



TOC